This article was downloaded by: [Tomsk State University of Control Systems and Radio]
On: 17 February 2013, At: 06:13
Publisher: Taylor & Francis
Informa Ltd Registered in England and Wales Registered Number: 1072954 Registered office: Mortimer House, 37-41 Mortimer Street, London W1T 3JH, UK

Molecular Crystals
Publication details, including instructions for authors and subscription information:
http://www.tandfonline.com/loi/gmcl15

Influence of Exciton Phonon Interaction on Metallic Reflection from Molecular Crystals

Bruno M. Fanconi [a b], George A. Gerhold [a b] & William T. Simpson [a b]
[a] Department of Chemistry, University of California, Davis, California
[b] Department of Chemistry, Institute of Theoretical Science University of Oregon, Eugene, Oregon

Version of record first published: 21 Mar 2007.

To cite this article: Bruno M. Fanconi , George A. Gerhold & William T. Simpson (1969): Influence of Exciton Phonon Interaction on Metallic Reflection from Molecular Crystals, Molecular Crystals, 6:1, 41-81

To link to this article: http://dx.doi.org/10.1080/15421406908082952

PLEASE SCROLL DOWN FOR ARTICLE

Full terms and conditions of use: http://www.tandfonline.com/page/terms-and-conditions

This article may be used for research, teaching, and private study purposes. Any substantial or systematic reproduction, redistribution, reselling, loan, sub-licensing, systematic supply, or distribution in any form to anyone is expressly forbidden.

The publisher does not give any warranty express or implied or make any representation that the contents will be complete or accurate or up to date. The accuracy of any instructions, formulae, and drug doses should be independently verified with primary sources. The publisher shall not be liable for any loss, actions, claims, proceedings, demand, or costs or damages whatsoever or howsoever caused arising directly or indirectly in connection with or arising out of the use of this material.

Molecular Crystals and Liquid Crystals. 1969. Vol. 6, pp. 41–81
Copyright © 1969 Gordon and Breach Science Publishers
Printed in Great Britain

Influence of Exciton Phonon Interaction on Metallic Reflection from Molecular Crystals

BRUNO M. FANCONI, GEORGE A. GERHOLD and WILLIAM T. SIMPSON

Department of Chemistry, University of California, Davis, California

and

Department of Chemistry and Institute of Theoretical Science
University of Oregon, Eugene, Oregon

Received January 9, 1969, *in revised form April* 7, 1969

Abstract—Reflection spectra of a number of polymethine dyes are presented and analysed. Characteristic features of these spectra appear to be outside the framework of the Lorentz–Lorenz theory. An alternate approach based on an appropriate linear response function for surface excitation is developed. The linear response at a particular frequency involves a sum over all k-dependent Green's functions. Damping is brought in through the exciton–phonon interaction. A model Hamiltonian is introduced which can be diagonalized exactly for the single molecule. For the crystal, this permits the treatment of single phonon effects in the strong coupling limit almost as if they were multiple phonon effects. Structure, mainly associated with damping, in the reflection spectrum is expected and found in those regions of the exciton dispersion curve where the density of momentum states is large. Reasonably good agreement is found between the theoretical and experimental reflection curves.

1. Introduction and Experimental Results

The Lorentz–Lorenz formula without damping leads to a prediction that n, the refractive index, is purely imaginary in certain regions of the spectrum. A consequence is metallic reflection. This is not usually encountered experimentally with molecular crystals (in the visible and near ultraviolet) because, with typical physical

Downloaded by [Tomsk State University of Control Systems and Radio] at 06:13 17 February 2013

constants, the damping is important. To be more explicit, for a two level model described by

$$\frac{n^2-1}{n^2+2} = \frac{1}{3}\frac{\omega_p^2}{\omega_0^2 - \omega^2 + i\Gamma\omega}$$

the condition $\Gamma \ll \omega_p^2/2\omega_0$ gives an imaginary n over a band from $\omega_- = \omega_0 - \frac{1}{3}(\omega_p^2/2\omega_0)$ to $\omega_+ = \omega_0 + \frac{2}{3}(\omega_p^2/2\omega_0)$. However, for ordinary oscillator strengths and typical Γ's (Γ turns out to characterize the range of vibronic levels reached in the transition for isolated molecules) $\Gamma \gg \omega_p^2/2\omega_0$, and the same formula gives a standard anomalous dispersion curve with a band width Γ. The reflection coefficient is related to n by

$$R = \frac{|n-1|^2}{|n+1|^2}$$

In the former case this leads to metallic reflection. In the latter more usual case the reflectance is predicted to rise and then fall around ω_0, as is observed.

In an earlier study reflectance measurements revealed regions of metallic reflection for several molecular crystals, all of which had molecular transitions in these regions with comparatively enormous oscillator strengths[1]. These effects could be and were interpreted along the lines indicated above with moderate but incomplete success.

A development of the theory of the refractive index (often called the Hopfield–Fano theory[2,3] fits in with these experiments quite well in that the theory emphasizes the existence of stationary states—combinations of exciton and photon unperturbed states. It is a theory in which damping is initially ignored and according to which the stationary states have a dispersion relation $\omega(k)$ as shown in Fig. 1. The solid curves are the energies of the mixed states; the dotted lines are the unperturbed energies. The asymptotes come essentially at ω_- and ω_+ as defined above, and the region between has no stationary states (normal modes). This lack of normal modes directly causes metallic reflectance.

Downloaded by [Tomsk State University of Control Systems and Radio] at 06:13 17 February 2013

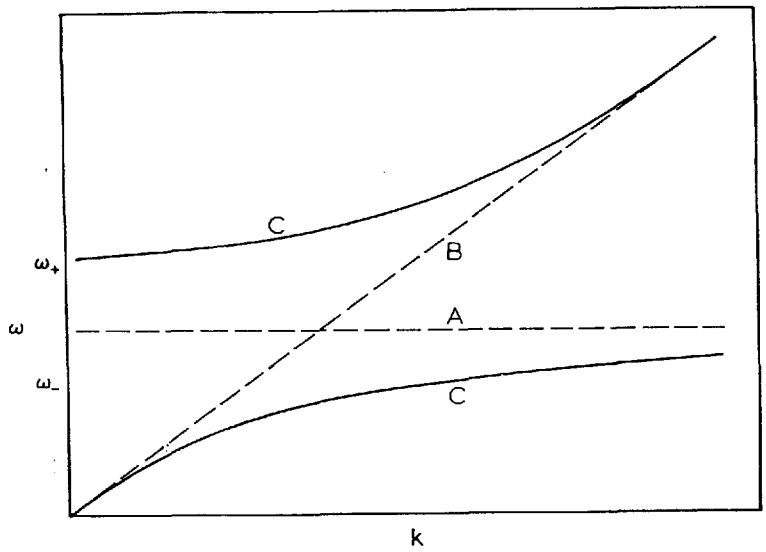

Figure 1. Dispersion curves for a two level system. (A) dispersion curve for uncoupled molecules; (B) dispersion curve for radiation; (C) dispersion curves for the coupled system. ω_+ and ω_- designate the limits of the region free from normal modes in the coupled system.

In the present research we shall still be concerned with the case $\Gamma \ll \omega_p^2/2\omega_0$, the one for which metallic reflectance occurs; but we shall now be focusing more closely on details of the experimental results to attempt to delineate what must be the effects of damping —or, to anticipate, the effects of the phonon interaction.

After studying a series of room temperature reflection curves, one taken at 4°K, and a pertinent absorption curve, we shall attempt to fit these spectra with the Lorentz–Lorenz formula with damping. Finding that this is not entirely satisfactory we are led to regard things in the spirit of the Hopfield–Fano theory. Accordingly we shall be developing a quantal theory of the damping. The approach will be to introduce the phonon interaction and its effect by way of the Fourier transform of an appropriately selected, zero temperature, double-time Green's function. The results of this quantal treatment seem to agree

Downloaded by [Tomsk State University of Control Systems and Radio] at 06:13 17 February 2013

reasonably well with what is observed, but certainly some questions remain.

Apparatus. The reflection spectrometer used for the room temperature spectra has been modified from an earlier design.[1] Significant improvements in accuracy and convenience have been achieved by addition of a second beam with matched optics and a standard mirror. The half-silvered quartz plate which served as a beam splitter has been replaced by a thin quartz coverslip in order to minimize the separation between the multiple images formed by unwanted reflections at the beam splitter. Replacement of the phototube by a microscope eyepiece permits detailed examination of the crystal face to be studied; if the phototube is positioned correctly, this can be done without refocussing. The crystal is mounted on a two circle goniometer; both the goniometer and the standard mirror are fixed on two kinematic stages which are stacked with their degrees of freedom parallel and perpendicular to the optical axis respectively. The crystal face in question is rotated normal to the incident beam via the goniometer arcs, and the principal directions of the face are matched with those of a fixed polarizer by rotation of the whole goniometer. The spectra were obtained by alternately measuring the intensity from the crystal and the standard mirror. Correction was made for light reflected by the lenses and for imperfections in the standard mirror; the standard mirror was calibrated on an instrument based on a design of Haas,[4]

The low temperature spectrometer is quite similar to our original single beam instrument. The problem of windows and long working distance, which are inseparable from liquid helium dewars, were overcome with a lens–mirror combination designed by Dyson.[5] The combination of this device and a Carl Zeiss 6 mm quartz monochromat is essentially achromatic in the visible and near ultraviolet. The crystal was glued (G.E. 4031) onto a copper rod in contact with the helium reservoir. No attempt was made to measure the temperature at the crystal, but there was no evidence of change in the spectrum after long equilibration times. Experience with cooling arrangements of this nature

Downloaded by [Tomsk State University of Control Systems and Radio] at 06:13 17 February 2013

shows that the He B.P. may have been exceeded by several degrees.

The single crystal absorption spectrum was measured on an instrument of standard design. Light from a monochromator was focused on a crystal mounted over a pinhole with a microscope objective. A second objective was used to collect and collimate the transmitted light for the polarizer and the phototube.

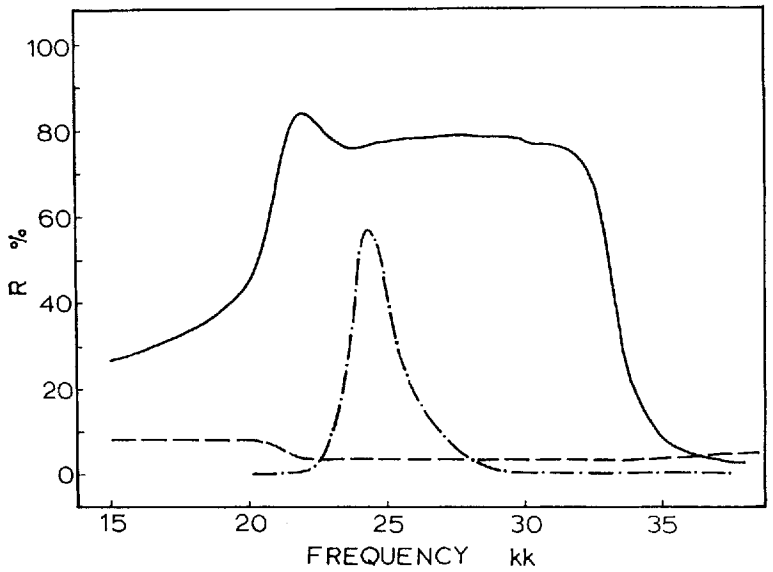

Figure 2. Crystal reflection spectra for the prominent face of 1,5-*bis*-(dimethylamino) pentamethinium perchlorate obtained with light polarized along two principal directions (—) and (– – –), and the absorption spectrum of the same compound in water (– · – ·). [Reproduced from (1).]

Results. The earlier study of metallic reflection in molecular crystals was primarily concerned with an explanation of the gross features of the spectrum of 1,5-*bis*-(dimethylamino)-pentamethinium perchlorate (BDP) shown in Fig. 2.[1] Although these gross features—the existence, position, width and average height[1] of the metallic band—are contained within the simple Lorentz–Lorenz approach, the spectrum shows many additional features

Downloaded by [Tomsk State University of Control Systems and Radio] at 06:13 17 February 2013

which must be explained by an extended theory. The only extensions possible within the Lorentz–Lorenz framework are modification of the internal field effect and/or the introduction of multiple vibronic transitions each with its own damping constant. These contributions should be considerably easier to delineate at low temperatures; the appropriate spectra of BDP are shown in Fig. 3. Comparison of the two spectra shows that the changes

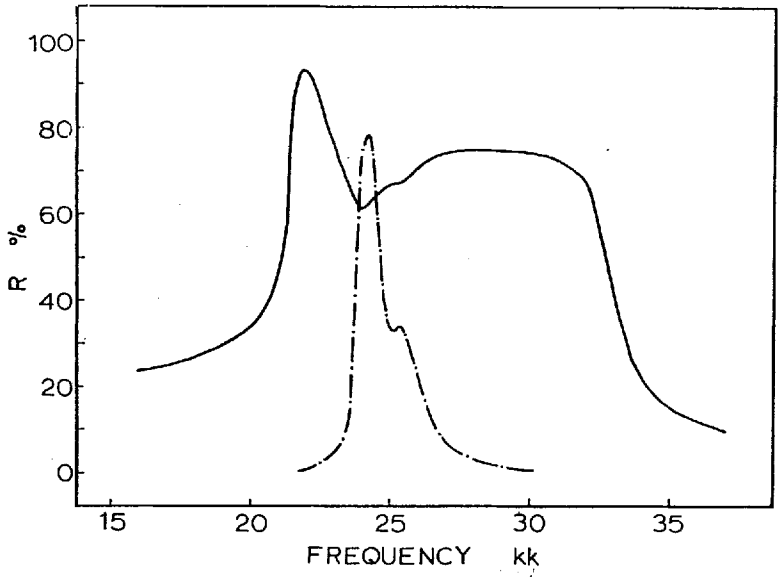

Figure 3. Low temperature (4 °K) crystal reflection spectrum for the prominent face of 1,5-*bis*-(dimethylamino)pentamethinium perchlorate obtained with light polarized along the principal direction of maximum reflection (—), and the absorption spectrum of the same compound in a 7–3 isobutanol-isopentane glass at about 77 °K (– · – ·).

are rather minor. Specifically, there is a slight steepening of the band edges, a small red shift of the blue edge of the band, and a new bit of structure around 25.5 kK in both the reflection and single-molecule absorption spectra. We shall be attempting to focus on those features which are beyond the realm of the simple Lorentz–Lorenz formula and shall not hesitate, henceforth, to

Downloaded by [Tomsk State University of Control Systems and Radio] at 06:13 17 February 2013

look at room temperature reflectances. For the spectra of BDP in Fig. 2 and 3 the features on which we shall concentrate are the abruptness of the band edges, the deviations from perfect reflections within the band, the structure within the band, and the very low reflectivity in the region around 40 kK (the single molecule absorption in this region implies a conventional reflection band with a reflectivity of 15–20%).

Using the Lorentz–Lorenz formula one finds that the abrupt band edges can only be reproduced by introduction of a damping constant which is at least an order of magnitude less than the single molecule half-width, but unfortunately this damping constant also leads to almost perfect ($> 99\%$) reflection throughout the band. It is evident that the dissipative processes (and thus Γ) must be strongly frequency dependent if we are to reproduce the observed spectra. There is always a region of low reflectance between the transitions in a two term Lorentz–Lorenz formula. Consequently the structure around ω_0 can be reproduced by dividing the single molecule absorption into a large number of transitions (25 were tried) with very small damping constants (about 1/20th of the distance between transitions). The position of this structure relative to the band edges is controlled by the internal field. Fig. 4 illustrates this fact for the two-transition case—where reflection curves are shown calculated for representative parameters which characterize the contribution of the internal field. It is seen that the dip is fixed whereas the band is shifted by the effect of the internal field. This means that the structure at the red end of metallic reflection bands (assumed to be associated with molecular transitions) should always come at ω_0. This prediction seems to be fulfilled for the spectrum in Fig. 3, but examination of the spectrum in Fig. 2 shows that the minimum in the reflection band is displaced about 0.6 kK to the red from the maximum of the single molecule absorption. What is meant by "single molecule absorption" is of course a bit ambiguous (solvent shifts).

The question of the relative positions of the structured zones within the band, the single molecule absorption, and the band

Downloaded by [Tomsk State University of Control Systems and Radio] at 06:13 17 February 2013

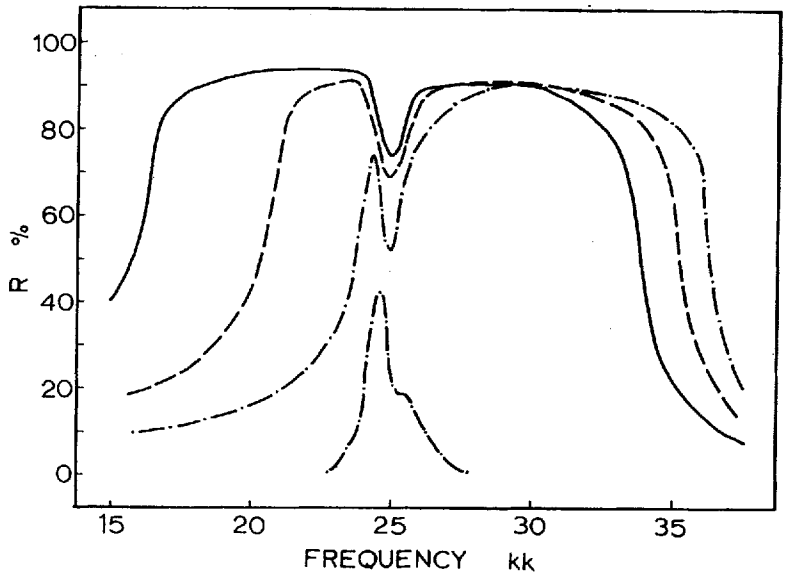

Figure 4. Effect of the internal field on reflection spectra calculated from a two-transition Lorentz–Lorenz formula.

$\omega_1 = 24.4$ kK $\quad \gamma_1 = .4$ kK $\quad f_1 = 2.16$

$\omega_2 = 25.6$ kK $\quad \gamma_2 = .7$ kK $\quad f_2 = 1.16$

(—) internal field $= 4/3\pi$; (– – –) internal field $= 2\pi/3$; (– · – ·) internal field $= 0$ (Sellmeier); and an approximate absorption spectrum (– · – ·).

edges is a crucial one. We consider next a series of metallic reflection spectra which almost certainly involve a variety of internal fields. The spectra shown in Fig. 5–9 all agree in their gross features with predictions based on the Lorentz–Lorenz formula, but they also show in varying degrees features which do not agree with that simple theory. With this set of spectra we can make several generalizations. If a broad metallic reflection band is present, the blue edge of this band is sharp and much the same from one spectrum to another. If large dips occur (as in Figs. 2, 3, 6, and 7), they always begin near the red end of the band, that is, close to ω_- (not with the low frequency edge of the

Downloaded by [Tomsk State University of Control Systems and Radio] at 06:13 17 February 2013

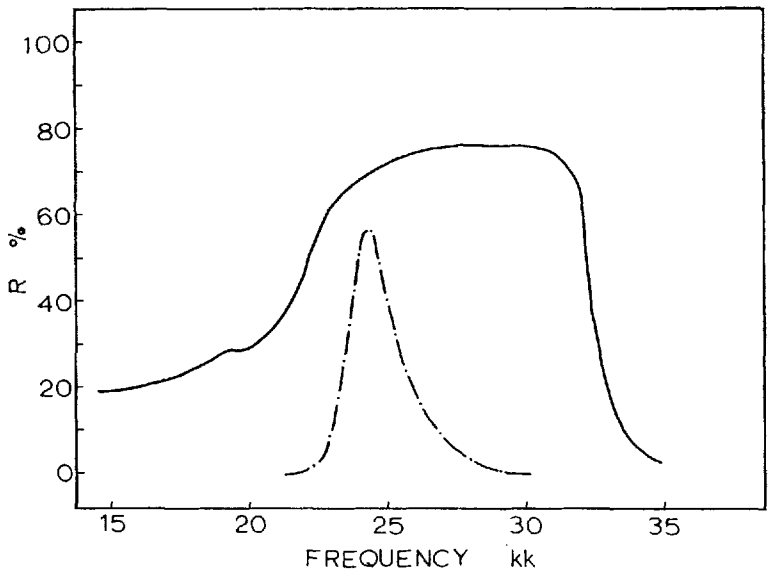

Figure 5. Crystal reflection spectrum of a minor face of 1,5-*bis*-(dimethylamino)pentamethinium perchlorate obtained with light polarized along the principal direction of maximum reflection (—), and the absorption spectrum of the same compound in water (– · – · –).

corresponding single molecule transition ω_0).‡ Reflection in the region to the blue of the metallic band is anomalously low.

On the other hand there are also significant differences among these spectra. The red shift of the dip relative to the maximum in the single molecule absorption already noted in Fig. 2 is evident in Figs. 6 and 7. In the latter spectrum, which is a most important one for our present purposes, the dip begins rather far (2 kK) to the red of the onset of the single molecule absorption. It appears

‡ An indirect but striking example of the fact that the absorption is associated with ω_- not ω_0 is the following: whereas the single molecule fluorescence of BDP comes at 429 mμ (20 mμ to the red of the absorption at 409) the fluorescence of crystalline BDP iodide peaks at 510 mμ, 20 mμ to the red of the 490 mμ region, a region where there is a dip in reflectance presumably corresponding to the greatest damping and/or absorption (Fig. 9).

Downloaded by [Tomsk State University of Control Systems and Radio] at 06:13 17 February 2013

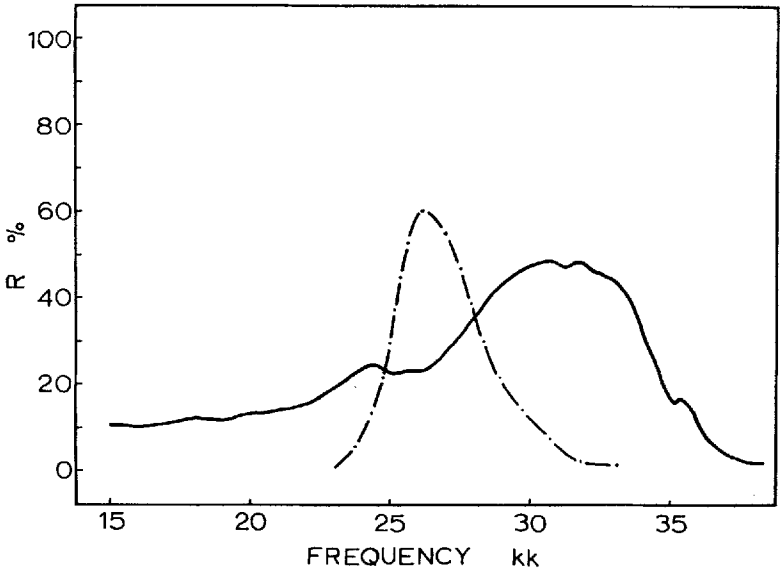

Figure 6. Crystal reflection spectrum of one face of 5-N-methylanilino-2,4-pentadienal obtained with light polarized along the direction of maximum reflection (—), and the absorption spectrum of the same compound in methanol (– · – ·). [Reproduced from (1).]

that, in contradiction to the results from the Lorentz–Lorenz formula (Fig. 4) the position of the dip (at least the start of it) is related to ω_- rather than to ω_0, and thus is dependent on the internal field! If we adopt this viewpoint, the rather featureless metallic bands in Figs. 8 and 9 can be described as analogs of those in Figs. 2 and 7, but in which the dip is either broader or closer to ω_- than " normal ". We then presume that the dissipative processes which are associated with the dip suppress the reflectance sufficiently to eliminate the sharp spike at ω_-; the comparatively gentle rise in reflectance on the red end of the metallic band is then analogous not to the 20–21.5 kK region of the spectrum in Fig. 3, but rather to the 24–27 kK region. The metallic bands in Figs. 5 and 6 are apparently intermediate cases in which the spike is not completely suppressed, as is indicated

Downloaded by [Tomsk State University of Control Systems and Radio] at 06:13 17 February 2013

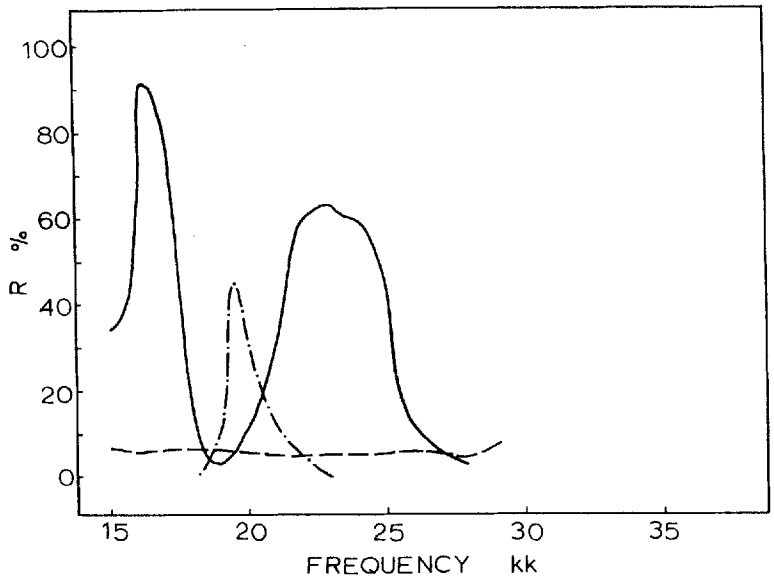

Figure 7. Crystal reflection spectrum of one face of the red crystal form of 4-acetoxy-1,7-*bis*-(dimethylamino)heptamethinium iodide obtained with light polarized along the two principal directions (—) and (– – –) and the absorption spectrum of the same compound in ethanol (– · – ·).

by the structure at 19.5 kK and 24.3 kK respectively.‡ The foregoing analysis indicates that the dip can be quite distant from ω_0; for the spectra in Figs. 5, 8, and 9 this displacement is approximately 3 kK. Because of arguments like the foregoing we are led to conclude that the detailed shapes and heights of these metallic reflection bands cannot be reproduced within the Lorentz–Lorenz framework, and that to clear up the discrepancies would require a microscopic theory of damping.

There are some additional experimental results. Several of the spectra show a small but unmistakable dip on the top of the metallic band near ω_+. This is quite evident in Fig. 2 (at 30.2 kK) and Fig. 7 (at 23.4 kK), but less certain in Fig. 6. Its absence in

‡ A similar feature is barely detectable in Fig. 9 at 20.5 kK.

Downloaded by [Tomsk State University of Control Systems and Radio] at 06:13 17 February 2013

Fig. 3 is not significant because of a rather high experimental error in this spectral region (low temperature spectrometer). What is more, there is an absorption peak right around ω_+, at least for thin crystals (Fig. 10).

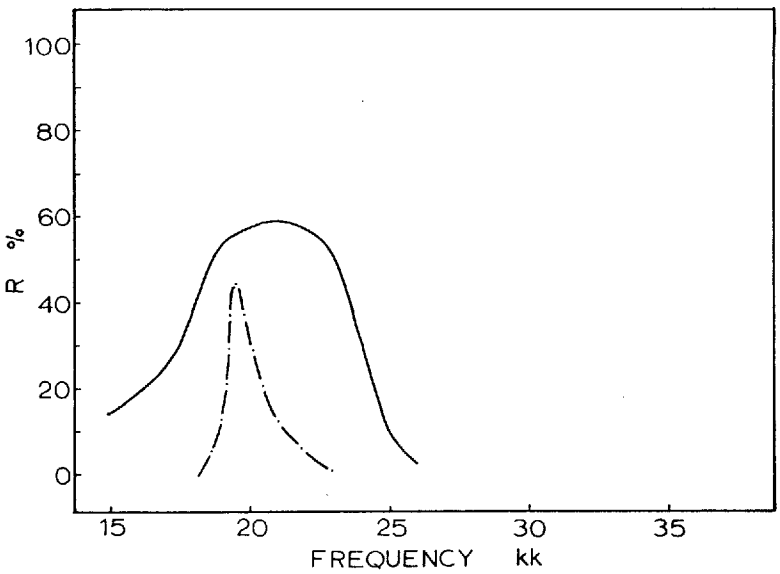

Figure 8. Crystal reflection spectrum of one face of the blue crystal form of 4-acetoxy-1,7-*bis*-(dimethylamino)heptamethinium iodide obtained with light polarized along the principal direction of maximum reflection (—), and the absorption spectrum of the same compound in ethanol (– · – ·).

In the next two sections the aim will be to lay the theoretical groundwork for an eventual explanation of many‡ of the observations recorded and generalized in the foregoing. The next section has to do with the calculation of the susceptibility, and hence the reflectivity; and the one after with adoption of a model Hamiltonian deemed to bring in the phonon interaction in a reasonable way.

‡ We have found no explanation for the small dip, e.g. at 30.2 in Fig. 2.

Downloaded by [Tomsk State University of Control Systems and Radio] at 06:13 17 February 2013

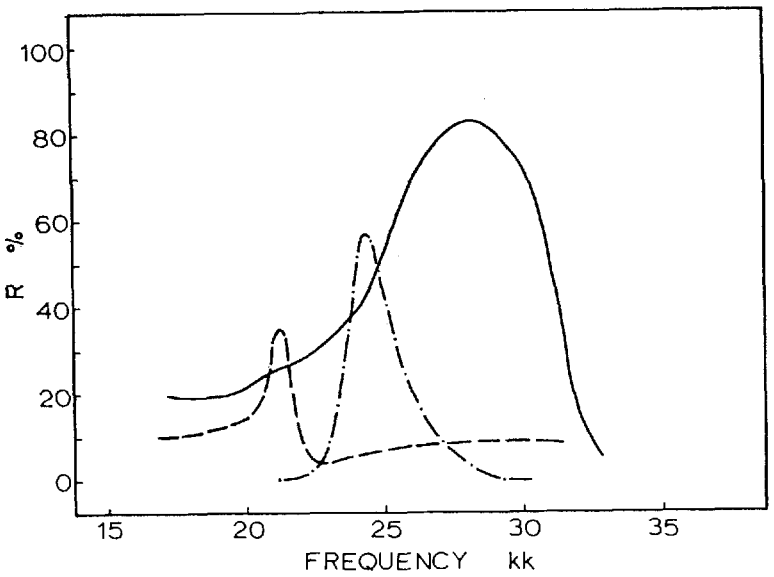

Figure 9. Crystal reflection spectrum of one face of 1,5-*bis*-(dimethylamino) pentamethinium iodide obtained with light polarized along the two principal directions (—) and (– – –), and the absorption spectrum of the same compound in water (– · – · ·).

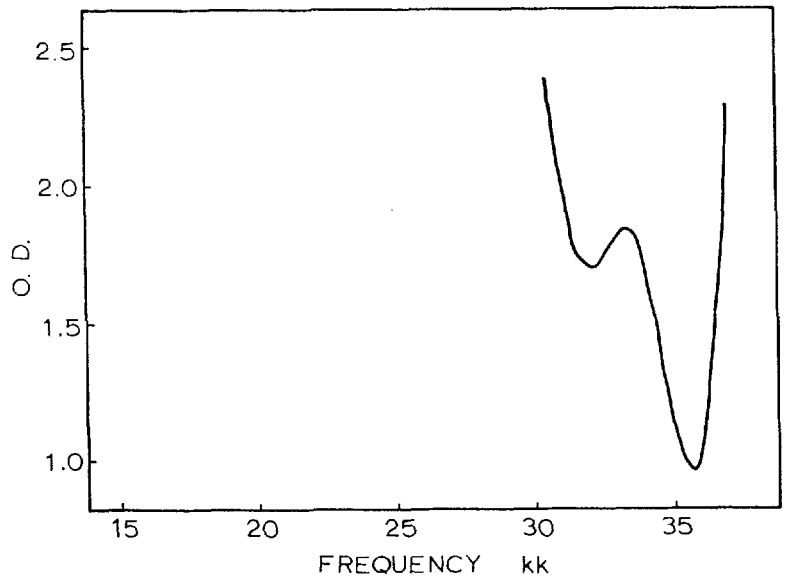

Figure 10. Absorption spectrum of the prominent face of 1,5-*bis*-

Downloaded by [Tomsk State University of Control Systems and Radio] at 06:13 17 February 2013

Downloaded by [Tomsk State University of Control Systems and Radio] at 06:13 17 February 2013

2. Complex Susceptibility Formalism

In this section the main aim will be to connect the Fourier transform of the so-called double-time Green's function over excitation operators with a susceptibility function appropriate for the study of metallic reflection. The connection will be made through the calculation of the linear response.[6a,6]

The response will be taken as a ground state matrix element of the electric moment operator—the state having developed from $t = -\infty$ up to $\bar{t}$. A selected molecule, the rth, will have a moment determined by the interaction between it, the external field, and the other molecules (themselves generally affected by the field and their mutual interaction). The state $|\bar{t}\rangle$ is developed from the initial state by the time development operator

$$|\bar{t}\rangle = u(\bar{t}, -\infty)\,|-\infty\rangle$$

where

$$u(\bar{t}, -\infty) = 1 - i\int_{-\infty}^{\bar{t}} H_{\text{int}}(t)\,dt - \int_{-\infty}^{\bar{t}} H_{\text{int}}(t)\,dt \int_{-\infty}^{t} H_{\text{int}}(t')\,dt' + \cdots$$

We use the natural units $\hbar = 1$.

Retaining only those terms linear in the interaction in $u(t, -\infty)$ the contribution to the response from the rth molecule becomes

$$\langle \bar{t}\,|\,\mu_r\,|\,\bar{t}\rangle = \langle -\infty\,|\,\mu_r\,|\,-\infty\rangle + i\int_{-\infty}^{\bar{t}} \langle -\infty\,|\,[\mu_r(\bar{t}), H_{\text{int}}(t)]\,|\,-\infty\rangle\,dt$$

The time dependence is, for our purposes, governed by an

$$H_{\text{int}}(t) = \sum_p \epsilon_p(t) \cdot \sum_{\text{in}\,p,\nu} q_\nu \mathbf{x}_\nu(t) \equiv \sum_p \epsilon_p(t)\mu_p(t)$$

the q's being the charges, and $\epsilon_p(t)$ the value of the external or driving field at the pth molecule at the time t. The commutator arises from the complex conjugate parts of the matrix element. The $\mu_r(t)$ are operators in interaction representation considering the solid as the unperturbed system and $\epsilon(t)$ as supplying the perturbation. This makes the μ's operators in Heisenberg

representation with respect to a treatment of the solid in the absence of an external field. The external field is being considered classically. It is convenient to write this contribution to the response as

$$\Delta\mu_r(\bar{t}) = i\sum_p \int_{-\infty}^{\bar{t}} dt\, \epsilon_p(t)\langle [\mu_r(\bar{t}), \mu_p(t)]\rangle \tag{1}$$

to present a picture of an induced dipole which oscillates about a zero value, the molecules having no permanent dipole moment. The Dirac brackets signify ground-state expectation-value.

For definiteness, let us consider $\epsilon(t)$ as associated with a light beam propagating along z and polarized y. The solid will be considered to have molecules at the corners of a cubic lattice with transition moments y. Now we shall adopt a special numbering system for a molecule which uses two subscripts: the first, which is like z, to give the number of a plane ($\perp$ to z) and the second to give the position in the plane. Instead of μ_r we have μ_{sa} where $s = 1 \to S$ and $a = 1 \to A$. S is the number of planes and A the number in a plane. For one cubic centimeter, as will be assumed here, N (molecules per cc.) also satisfies

$$SA = N$$

The average response in the front surface when considered as a polarization brings in N

$$\Delta P(z = 0) = N\Delta\mu_{1a}$$

At this point we make a seemingly drastic assumption, namely that the radiation which has a wavelength the same as in vacuo fails to penetrate past the front surface—this because of the extinction theorem. To pay the consequences of this assumption (and now expressing ourselves in a language related to Coulomb gauge) we must not forsake the consideration of the transverse **A** field in treating the bulk solid. Thus, for the mutual interactions of the molecules we shall be using the retarded Coulomb interaction. The complicated in-depth effects are all contained

Downloaded by [Tomsk State University of Control Systems and Radio] at 06:13 17 February 2013

in the μ's—this because the μ's are Heisenberg operators and so are governed by the Hamiltonian for the solid.

The response (1) may now be rewritten using

$$\epsilon_{sa} = \epsilon_{sa}\,\delta_{s1} \quad \text{and} \quad \epsilon_{1a} = \epsilon(z=0) = f\cos\omega t$$

For the rth molecule in the front surface $r \to 1a'$

$$\Delta P(z=0) = i\,N f \sum_a \int_{-\infty}^{\bar{t}} dt\,\cos\omega t \langle[\mu_{1a'}(\bar{t}), \mu_{1a}(t)]\rangle$$

Moreover, $\sum_a [\mu_{1a'}(\bar{t}), \mu_{1a}(t)]$ is independent of the position of a' so we can equally well use

$$\Delta P(z=0) = i\frac{N}{A} f \sum_{a'}\sum_a \int_{-\infty}^{\bar{t}} dt\,\cos\omega t \langle[\mu_{1a'}(\bar{t}), \mu_{1a}(t)]\rangle \qquad (2)$$

The in-depth effects are still present owing to $\bar{t} - t$ having a finite value.

Now to digress for notational purposes: a single exciton having a " momentum is related to ones having different positions thus

$$b_{\mathbf{k}}^\dagger \mid 0\rangle = \frac{1}{\sqrt{N}} \sum_{p=1}^{N} e^{i\mathbf{k}\cdot\mathbf{r}_p} b_p^\dagger \mid 0\rangle$$

Here $b_p^\dagger$ is an Agranovitch excitation operator.[6a] It, working on the exciton " vacuum " $\mid 0\rangle$, makes an excitation at p ($\mid 0\rangle$ means all molecules are in their ground state). Also for a plane $s \perp z$ we have

$$b_{s\mathbf{k}}^\dagger \mid 0\rangle = \frac{1}{\sqrt{A}} \sum_{q=1}^{A} e^{i(k_x x_q + k_y y_q)} b_{sq}^\dagger \mid 0\rangle$$

where $\mathbf{k}$ is understood as having x and y components only. In this restricted sense the $k = 0$ mode becomes

$$b_{s0}^\dagger \mid 0\rangle = \frac{1}{\sqrt{A}} \sum_{q=1}^{A} b_{sq}^\dagger \mid 0\rangle$$

In the same way we define ($\mid g\rangle$ the true ground state)

$$\mu_{s0} \mid g\rangle = \frac{1}{\sqrt{A}} \sum_{q=1}^{A} \mu_{sq} \mid g\rangle$$

Downloaded by [Tomsk State University of Control Systems and Radio] at 06:13 17 February 2013

and in particular ($s = 1$ for the front surface)

$$\langle g \mid \mu_{10}(\bar{t}) = \frac{1}{\sqrt{A}} \sum_{a'=1}^{A} \langle g \mid \mu_{1a'}(\bar{t})$$

Returning to the development of the response function we can now modify the LHS of (2) to read

$$\frac{iNf\sqrt{A}}{A} \sum_{a} \int_{-\infty}^{\bar{t}} dt \cos \omega t \langle [\mu_{10}(\bar{t}), \mu_{1a}(t)] \rangle$$

and, repeating the process, to

$$\Delta P(z = 0) = iNf \int_{-\infty}^{\bar{t}} dt \cos \omega t \langle [\mu_{10}(\bar{t}), \mu_{10}(t)] \rangle \tag{3}$$

Note that subscript 1 stands for $z = 0$ (first layer), subscript 0 for $k_x = k_y = 0$. Again for notational purposes, a z-momentum exciton is

$$b_{k0}^{\dagger} \mid 0\rangle = \frac{1}{\sqrt{S}} \sum_{s=1}^{S} e^{ikz_s} b_{s0}^{\dagger} \mid 0\rangle$$

with inverse

$$b_{s0}^{\dagger} \mid 0\rangle = \frac{1}{\sqrt{S}} \sum_{|k|=0}^{S/2} e^{-ikz_s} b_{k0}^{\dagger} \mid 0\rangle$$

(The scalar k means k_z.)

Arguing similarly, and using $z_1 = 0$ for $s = 1$

$$\mu_{10} \mid g\rangle = \sqrt{\frac{A}{N}} \sum_{k|=0}^{S/2} \mu_{k0} \mid g\rangle$$

With this (3) becomes

$$\Delta P(z = 0) = ifA \sum_{k',k} \int_{-\infty}^{\bar{t}} dt \cos wt \langle (\mu_{k0}(\bar{t}), \mu_{k'0}(t)] \rangle$$

which, with conservation of momentum, acquires a factor $\delta_{k'\cdot k}$.‡

‡ Terms in the Hamiltonian for the solid which fail to conserve exciton momentum bring in phonon momenta. The phonon momentum terms have zero expectation value over the ground state in a zero temperature treatment.

Downloaded by [Tomsk State University of Control Systems and Radio] at 06:13 17 February 2013

Finally, with the abbreviation

$$G_k(\bar{t}, t) = i\langle[\mu_{k0}(\bar{t}), \mu_{k0}(t)]\rangle \tag{4a}$$

(the single k means k_z as in the foregoing).

We obtain

$$\Delta P(z = 0) = fA \sum_k \int_{-\infty}^{\bar{t}} dt \cos \omega t \, G_k(\bar{t}, t) \tag{4b}$$

Our result (4b) for $\Delta Pz = 0)$ at $\bar{t}$ contains a sinusoidal driving field $f \cos \omega t$ as a factor and would therefore (linear response) also be sinusoidal with the same frequency, but not necessarily the same phase. The susceptibility involves the proportionality between $\Delta P(\bar{t})$ and $\epsilon(\bar{t})$. To formalize this we write

$$\epsilon(\bar{t}) = f \cos \omega \bar{t}$$

$$\Delta P(\bar{t}) = \chi' f \cos \omega \bar{t} + \chi'' f \sin \omega \bar{t} \tag{5a}$$

so that e.g. if $\chi'' = 0$, $\Delta P(\bar{t})/\epsilon(\bar{t}) = \chi'$.

Note that also (5a) can be written

$$\Delta P(\bar{t}) = \mathrm{Re}[f(\chi' - i\chi'')(\cos \omega \bar{t} + i \sin \omega \bar{t})] = \mathrm{Re}\, f\chi \, e^{i\omega \bar{t}} \tag{5b}$$

where

$$\chi = \chi' - i\chi'' \tag{5c}$$

At this point we have two expressions for ΔP, (4b) and (5a), and must bring them together.‡ With $\tau = \bar{t} - t$ (4b) becomes

$$\Delta P(t) = -fA \sum_k \int_{\infty}^{0} d\tau \cos \omega(\bar{t} - \tau) \, G_k(\bar{t}, \bar{t} - \tau)$$

$$= fA \sum_k \int_{-\infty}^{\infty} d\tau \cos \omega(\bar{t} - \tau) \, G_k(\tau, 0)\theta(\tau)$$

Here $\theta(\tau)$ is the Heaviside function, and use has been made of the fact that only the difference between the two times in G matters—this because no external fields are involved in the expression 4a. With incorporation of a trigonometric identity this becomes

‡ This treatment is based on notes by Yo Han Pao. We are grateful to Professor Pao for showing us these notes.

Downloaded by [Tomsk State University of Control Systems and Radio] at 06:13 17 February 2013

$$\Delta P(\bar{t}) = fA \sum_k \int_{-\infty}^{\infty} d\tau \, [G_k(\tau, 0)\,\theta(\tau) \cos \omega\tau \cos \omega\bar{t} + G_k(\tau, 0)\,\theta(\tau) \sin \omega\tau \sin \omega\bar{t}]$$

Now comparing with (5a) we have

$$\chi' = A \sum_k \int_{-\infty}^{\infty} d\tau \, G_k(\tau, 0)\, \theta(\tau) \cos \omega\tau$$

$$\chi'' = A \sum_k \int_{-\infty}^{\infty} d\tau \, G_k(\tau, 0)\, \theta(\tau) \sin \omega\tau$$

Multiplying the second expression by i and adding we find

$$\chi^* = A \sum_k \int_{-\infty}^{\infty} d\tau \, G_k(\tau, 0)\, \theta(\tau)\, e^{i\omega\tau}$$

or using subscript ω for the Fourier transform

$$\chi^* = A \sum_{|k_z|=0}^{S/2} G_k(\tau, 0)\, \theta(\tau) \Big|_\omega \tag{6}$$

We have reached a stopping-place. However, for the special problem as defined in the next section, further simplification is possible and desirable. We begin by expressing the μ operators in the known way in terms of the excitation operators

$$\boldsymbol{\mu}_k = (\boldsymbol{\mu})(b_k + b_k^\dagger)$$

Here $(\boldsymbol{\mu})$ is the appropriate transition moment for a single molecule. For a y polarized transition, as assumed for definiteness above,

$$(\boldsymbol{\mu}) = \hat{y} \int \psi_{\text{ground}} \sum_\nu q_\nu y_\nu \psi_{\text{excited}}\, d\tau \equiv \hat{y}\mu_y$$

Thus $(\boldsymbol{\mu}) \cdot (\boldsymbol{\mu})$ is the number $,\mu_y^2$. In terms of excitation operators (4a) becomes

$$G_k(\tau,0) = i\mu_y^2 \langle [(b_k^\dagger(\tau) + b_k(\tau))(b_k^\dagger(0) + b_k(0)) - (b_k^\dagger(0) + b_k(0))(b_k^\dagger(\tau) + b_k(\tau))] \rangle$$

Downloaded by [Tomsk State University of Control Systems and Radio] at 06:13 17 February 2013

The reversal of the order in the commutator requires that the expectation value for the second part be the complex conjugate of the one for the first part. Thus

$$G_k(\tau, 0) = i\mu_y^2(2i)\ \mathrm{Im}\langle(b_k^\dagger(\tau) + b_k(\tau))(b_k^\dagger(0) + b_k(0))\rangle$$

For the model we shall be considering the ground state is the exciton vacuum $|\, g\rangle = |\, 0\rangle$. What is more, for the Hamiltonian we shall be using only one of the four terms is non-vanishing. It is the one

$$G_k(\tau, 0) = -\ 2\mu_y^2\ \mathrm{Im}\langle 0 \mid b_k(\tau)b_k^\dagger(0) \mid 0\rangle$$

We may now introduce the so-called double-time retarded Green's function

$$g_k(\tau, 0) \equiv -\ i\theta(\tau)\langle 0 \mid b_k(\tau)b_k^\dagger(0) \mid 0\rangle$$

(as with G, the single k here means k_z, where $k_x = k_y = 0$) so that

$$G_k(\tau, 0)\ \theta(\tau) = -\ 2\mu_y^2\ \mathrm{Im}(ig_k(\tau, 0)) = -\ 2\mu_y^2\ \mathrm{Re}\ g_k(\tau, 0)$$

and (6) can be written

$$\begin{aligned}\chi^* &= -\ 2\mu_y^2 A \sum_k \mathrm{Re}\ g_k(\tau, 0)\,|_\omega = -\ \mu_y^2 A \sum_k [g_k(\tau, 0) + g_k^*(\tau, 0)]\,|_\omega \\ &= -\ \mu_y^2 A \sum_k \{g_k(\tau, 0)\,|_\omega + [g_k(\tau, 0)\,|_{-\omega}]^*\} \qquad (7)\end{aligned}$$

The focus shifts to the computation of $g_k(\tau, 0)$ or, better, its transform. In the simple case of no dispersion

$$H = \omega_0 \sum_k b_k^\dagger b_k$$

it is readily shown that

$$g_k(\tau, 0)\,|_\omega = -\frac{1}{\omega_0 - \omega}$$

so that, using (7), we find

$$\chi^* = \mu_y^2 A \sum_{|k|=0}^{S/2} \left(\frac{1}{\omega_0 - \omega} + \frac{1}{\omega_0 + \omega}\right) = \frac{2\mu_y^2 N\omega_0}{\omega_0^2 - \omega^2}$$

Downloaded by [Tomsk State University of Control Systems and Radio] at 06:13 17 February 2013

If the Hamiltonian expressed in terms of momentum excitation operators has dispersion

$$H = \sum_k \omega_k b_k^\dagger b_k$$

but the bulk of the ω_k values are close to a single one, say ω_- (near, but not coinciding with ω_0) the result would be similar

$$\chi^* \approx \frac{2\mu_y^2 N\omega_-}{\omega_-^2 - \omega^2} \approx \frac{2\mu_y^2 N\omega_0}{\omega_-^2 - \omega^2} \tag{8a}$$

Now, the Lorentz–Lorenz relation for a two-level system without damping (standard internal field for a cubic crystal) may be written as a Sellmeier formula with a frequency shift

$$n^2 - 1 = \frac{\omega_p^2}{[\omega_0^2 - \frac{1}{3}\omega_p^2] - \omega^2}$$

The square of the plasma frequency $\omega_p^2 = 4\pi N(e^2/m)f$ with f given its quantum theoretical value becomes

$$\omega_p^2 = 8\pi\mu_y^2 N\omega_0$$

so the Lorentz–Lorenz formula is equivalent to

$$n^2 - 1 = 4\pi \frac{2\mu_y^2 N\omega_0}{[\omega_0^2 - \frac{1}{3}\omega_p^2] - \omega^2} \tag{8b}$$

We see that (8a) and (8b) can essentially be brought together if the calculated ω_-^2 should happen to coincide with $\omega_0^2 - \frac{1}{3}\omega_p^2$; in this eventuality one is then led to make the simple assumption

$$n^2 - 1 = 4\pi\chi^* \tag{9}$$

The dispersion relation used in this paper (Appendix B) based on Coulomb's law plus retardation indeed exhibits the desired coincidence (in Fig. 11, Section 3, the arrows indicate the ω_- and ω_+ of the stopping band as given by the Lorentz–Lorenz formula).‡

‡ A corollary, perhaps deserving more investigation, is that the ϵ appearing in our χ (say, the $\epsilon(\bar{t})$ in $\chi' = \Delta P(\bar{t})/\epsilon(\bar{t})$ for the front surface) would be not only an $\epsilon_{\text{effective}}$ for the response calculation but apparently also an ϵ_{true} as occurring in the $n^2 - 1$ of the macroscopic theory.

Downloaded by [Tomsk State University of Control Systems and Radio] at 06:13 17 February 2013

In consequence, we should expect to be able to use our χ^* (7) for calculating n, (9), and then this n for calculating the reflectance with

$$R = \frac{|n-1|^2}{|n+1|^2} \tag{10}$$

3. Exciton–Phonon Green's Function

Once we know the Green's functions we are in a position, combining (7), (9), and (10), to calculate reflectances. In this section we therefore concentrate on the calculation of the Fourier transform of g_k for arbitrary k. Our basic concern with the effect of molecular vibrations on metallic reflection in molecular crystals dictates our choice of Hamiltonian.

Our Hamiltonian may be expressed as a part representing isolated molecules and a part describing their interactions. Our tentative (and conventional) choice is $H_0 + H_1$

$$H_0 \sim \sum_p (\omega_0 b_p^\dagger b_p + \Delta v_p^\dagger v_p + \gamma(v_p^\dagger + v_p) b_p^\dagger b_p$$

$$H_1 \sim \sum_{p,r} \mu_y^2 T_{pr}(b_p^\dagger + b_p)(b_r^\dagger + b_r)$$

The v's for molecular vibration, are analogous to the b's except that one expects them to obey boson commutation rules (rather than the exciton commutation rules of the b's, characteristic of a two-level approach). Δ is the vibration frequency. In having only one type of v we are assuming that for the purposes of the model only one vibration is needed. The rationale of the γ-term is that electronic excitation causes a displacement in the equilibrium position but not a change in the force constant. The potential energy

$$V = \tfrac{1}{2}kQ^2 \xrightarrow{b^\dagger} \tfrac{1}{2}k(Q - Q_0)^2$$

The Q_0^2 term has no dynamical consequences and may be lumped

Downloaded by [Tomsk State University of Control Systems and Radio] at 06:13 17 February 2013

in with ω_0, which therefore refers to vertical excitation. The cross-term is

$$-kQ_0Q = -\Delta\left(\frac{m\Delta}{2}\right)^{1/2} Q_0(v^\dagger + v) \equiv \gamma(v^\dagger + v)$$

where m is the appropriate reduced mass.

The interaction will be retarded dipole–dipole[7] (for molecular crystals, by definition, as it were, one neglects exchange). The T_{pr} is the appropriate generalization of the static trigonometric factor

$$\frac{1 - 3\cos^2\theta}{R_{pr}^3} \to \left(\frac{\partial^2}{\partial x^2} + \frac{\partial^2}{\partial y^2}\right)\frac{e^{ik_0R_{pr}}}{R_{pr}} = T_{pr}$$

As used above μ_y^2 is a transition moment squared.

We shall begin with an important assumption, the neglect of differences in the effect of London forces as between the ground and excited states. This assumption gives us equality between the ground state and the exciton vacuum in the absence of an external field and eliminates troublesome divergences. Thus

$$H_1 = \sum_{p,r} \mu_y^2 T_{pr}(b_p^\dagger b_r + b_r^\dagger b_p) \tag{11}$$

With this H_1 and our tentative H_0 we have an H which can be transformed to momentum space (k and q subscripts)

$$H \sim \sum_{\mathbf{k}} \omega_{\mathbf{k}} b_{\mathbf{k}}^\dagger b_{\mathbf{k}} + \Delta \sum_{\mathbf{q}} v_{\mathbf{q}}^\dagger v_{\mathbf{q}} + \frac{\gamma}{\sqrt{N}} \sum_{\mathbf{k},\mathbf{q}} (v_{-\mathbf{q}}^\dagger + v_{\mathbf{q}}) b_{\mathbf{k}+\mathbf{q}}^\dagger b_{\mathbf{k}} \tag{12}$$

The part involving γ will be recognized as the so-called " Fröhlich terms "[8] in the superconductivity Hamiltonian.

Before getting on with our main task we bring in an alternate notation for the Fourier transform of $g_k(\tau, 0)$ (as in Eq. 7) again including the factor $-i\theta(\tau)$

$$g_k(\tau, 0)\,|_\omega \equiv \langle b_k(\tau) b_k^\dagger(0)\rangle_\omega \equiv -i\int_{-\infty}^{\infty} \theta(\tau)\langle b_k(\tau)\, b_k^\dagger(0)\rangle e^{i\omega\tau}\, d\tau$$

The ingredients of this (and more general) Green's functions are thus made manifest.

Downloaded by [Tomsk State University of Control Systems and Radio] at 06:13 17 February 2013

Conventionally, now, one takes the derivative with respect to τ of $g_k(\tau,0)$, one part of which involves the commutator with H; and afterwards one takes the transform to arrive at the following key expression

$$\omega\langle b_k(\tau)\, b_k^\dagger(0)\rangle_\omega = \langle b_k(0)\, b_k^\dagger(0)\rangle + \langle [b_k(\tau), H]\, b_k^\dagger(0)\rangle_\omega$$

After evaluation of the commutator one discovers a different g, and this g will be found to satisfy an equation similar to the one above. Repetition gives a process which may circle back on itself or may be open-ended. In the latter case it may be terminated artificially by some device such as the so-called de-coupling approximation or by a perturbation assumption. Our procedure will be to use a perturbation assumption because we are investigating exciton-phonon effects on metallic reflection, which puts us at the strong coupling limit (and allows us to ignore higher powers of γ^2/β where β is the width of the stopping band). If, in effect, we keep only γ^2 terms the process above involves only two equations in two kinds of g's. These equations can be solved using the tentative Hamiltonian (12) to give an equation which has a form the same as the one we shall be using, though not for the right reasons.‡

$$\langle b_k(\tau)\, b_k^\dagger(0)\rangle_\omega = 1\Big/\left(\omega - \omega_k - \frac{\gamma^2}{N}\sum_{\mathbf{k}} \frac{1}{\omega - \omega_{\mathbf{k}} - \Delta}\right) \qquad (13)$$

This equation reflects emission and absorption of but a single phonon. A multi-phonon approach would involve delaying termination of the process described above, and would give in place of (13) a continued fraction with Δ, 2Δ, 3Δ, ... successively. The present equation is only valid when the single-molecule electronic bandwidth is small compared with a typical vibrational quantum. Clearly this is not the case for electronic transitions in molecules.

To understand better the question of the range of validity we consider an equation similar to (13) derived using one of the

‡ Essentially the same equation was obtained by Suna[8] in the treatment of the exciton–phonon interaction for a one-dimensional (Einstein) crystal, using a variational approach.

Downloaded by [Tomsk State University of Control Systems and Radio] at 06:13 17 February 2013

independent parts of H_0 (no exciton hopping). When terms higher than γ^2 are ignored we find for a single molecule

$$\langle b(\tau) b^\dagger(0) \rangle_\omega = 1 \Big/ \left(\omega - \omega_0 - \frac{\gamma^2}{\omega - \omega_0 - \Delta} \right) \tag{14}$$

If the assumption $| \gamma | < \Delta$ is made, the frequencies come out to

$$\omega' \approx \omega_0 - \frac{\gamma^2}{\Delta}$$

$$\omega'' \approx \omega_0 + \Delta + \frac{\gamma^2}{\Delta}$$

and the intensities (from the residues)

$$I' = 1 - \frac{\gamma^2}{\Delta^2}$$

$$I'' = \frac{\gamma^2}{\Delta^2}$$

The difference $\omega'' - \omega' = \Delta$ (to first order), in agreement with the fact that the upper electronic state has the same force constant albeit a new equilibrium internuclear distance. Examination of the intensities shows that the " zero–zero " transition has almost all of the intensity, the other transition almost none. All of this is consistent and in agreement with expectation but physically unrealistic in the great majority of cases. Yet one would like to avoid the complications of a multi-phonon approach.

One gets the idea of turning things around, assuming $| \gamma | > \Delta$ which is physically the usual case ($| \gamma |$ could still be smaller than β). Then (14) gives two roots centered about ω_0 (which in any case is the frequency of the vertical transition). The splitting is no longer approximately Δ, the poles with Δ spacing having disappeared. In fact, now the scheme turns out to give a crude representation of the vibrational profile of the electronic band, a representation by two transitions with separation $2 | \gamma |$, and equal intensities.

By changing H_0 somewhat we can exploit this idea of using two levels to represent the band contour and can, at the same time,

Downloaded by [Tomsk State University of Control Systems and Radio] at 06:13 17 February 2013

keep the vibrational energy spacing constant at Δ before and after electronic excitation. To this end we represent the vibrational part with Pauli matrices (θ below is some parameter):

$$\frac{\Delta}{2}\{bb^\dagger\sigma_z + b^\dagger b(\sigma_x \sin\theta + \sigma_z \cos\theta)\} \tag{15a}$$

Putting in exciton commutation rules for the b's we find

$$\frac{\Delta}{2}\{\sigma_z + b^\dagger b(\sigma_x \sin\theta + \sigma_z(\cos\theta - 1))\} \tag{15b}$$

Whether the molecule is in its ground state ($bb^\dagger = 1$, $b^\dagger b = 0$) or in its excited state ($bb^\dagger = 0$, $b^\dagger b = 1$) the vibrational operator part is a Pauli matrix with eigenvalues ± 1 and splitting Δ. The case where $\theta \to 0$ resembles the one previously considered ($|\gamma| < \Delta$): the $b^\dagger b$ term (15b) becomes $(\theta\Delta/2)\sigma_x b^\dagger b$. Using v's as before except that now they satisfy exciton commutation rules this becomes $(\theta\Delta/2)(v^\dagger + v)b^\dagger b$, so that γ becomes $\theta\Delta/2$.

There was no necessity, however, to have made the demand $|\gamma| < \Delta$. Putting $\theta = 90°$ we obtain an extreme case in which the upper state vibrational states are represented by eigenvectors of σ_x. Thus the Frank–Condon integrals squared from the ground vibrational level of the ground electronic state are each one-half and the intensity is spread out as much as possible. Using $\sigma_z = 2v^\dagger v - 1$ we obtain in the $\theta = 90°$ case, now for one of the independent parts of H_0 (call it h_0)

$$h_0 \approx \bar{\omega}_0 b^\dagger b + \frac{\Delta}{2}(2v^\dagger v - 1)(1 - b^\dagger b) + \frac{\Delta}{2} b^\dagger b(v^\dagger + v)$$

$$= \bar{\omega}_0 b^\dagger b + \Delta v^\dagger v + \frac{\Delta}{2} b^\dagger b(v^\dagger + v) - \Delta v^\dagger v b^\dagger b - \frac{\Delta}{2}(1 - b^\dagger b)$$

or

$$h_0 + \frac{\Delta}{2} \approx \left(\bar{\omega}_0 + \frac{\Delta}{2}\right) b^\dagger b + \Delta v^\dagger v + \frac{\Delta}{2} b^\dagger b(v^\dagger + v) - \Delta v^\dagger v b^\dagger b$$

The key interaction term involving $b^\dagger b(v^\dagger + v)$ has $\Delta/2$ in place of γ; the electronic excitation has become $\bar{\omega}_0 + \Delta/2$ (which corresponds anyway to vertical excitation and fits our previous ω_0); there has been a shift in zero of energy which we can ignore,

Downloaded by [Tomsk State University of Control Systems and Radio] at 06:13 17 February 2013

and there is a new term $-\Delta v^\dagger v\, b^\dagger b$ which we cannot ignore. Our Hamiltonian for non-interacting molecules thus can be taken as involving the parts

$$H_0 = \sum_p \left[\omega_0 b_p^\dagger b_p + \Delta v_p^\dagger v_p + \frac{\Delta}{2} b_p^\dagger b_p (v_p^\dagger + v_p) \right] \tag{16a}$$

$$H_2 = -\Delta \sum_p v_p^\dagger v_p b_p^\dagger b_p \tag{16b}$$

Our model Hamiltonian uses (16) (exciton commutation rules for the v's as well as the b's) and (11)

$$H = H_0 + H_1 + H_2 \tag{17}$$

In momentum space the Hamiltonian has the same form as (12) with $\gamma/\sqrt{N}$ becoming $\Delta/2\sqrt{N}$ and with the extra term

$$H_2 = -\sum_{\mathbf{qkk'}} v_{\mathbf{q}}^\dagger v_{\mathbf{k+q+k'}} b_{\mathbf{k}}^\dagger b_{\mathbf{k'}}$$

The calculation of the Fourier transform of g with the v's obeying exciton commutation rules is a different story this time. The result analogous to and having the same form as (14) for the monomer is *exact*, because with only two vibrational levels multiphonon effects are out of the question. For the solid, multiphonon effects play a lesser role (no more than one phonon on a molecule at one time). As shown in Appendix A the one-phonon approximation leads to a dynamical equation the same as (13) ($\gamma \to \Delta/2$). The extra term has no effect at the level of the one-phonon approximation‡ and the validity of this approximation

‡ With regard to the effect of H_2 (16b) we have calculated numerically $g(\tau, 0)$ (not the transform) for the infinite one-dimensional polymer based on the full H (17). Graphs of g are trains of waves with component frequencies and strengths corresponding to the theoreticlly predicted spectrum. The graphs with and without H_2 show its effect to be a weak extra ripple with frequency *ca* ω_0. One can understand this physically from a careful consideration of a " collision " between a moving exciton and a stationary phonon. The exciton potential energy according to H_2 (16b) is lowered at the point of impact (exciton and phonon on the same molecule). We think of the terms in H_2 therefore as " trapping terms " and interpret the extra ripples in $g(\tau,0)$ in the one-dimensional example as meaning that the weak-coupling result (vibronic bands around ω_0) is making an incipient appearance.

Downloaded by [Tomsk State University of Control Systems and Radio] at 06:13 17 February 2013

turns out to depend on having the part

$$\frac{\Delta^2}{4N}\sum_{\mathbf{k}}\frac{1}{\omega-\omega_{\mathbf{k}}-\Delta}\equiv i\Gamma$$

be small with respect to the range of variation of $\omega_{\mathbf{k}}$. This last is essentially equivalent to our strong coupling assumption

$$\Gamma< \beta$$

(we are using β for $\omega_+ - \omega_- \approx \omega_p^2/2\omega_0 \approx 4\pi N\mu_y^2$)

Our stated aim in this section was to obtain the Fourier transform of g_k. This we consider to have been accomplished in that we have provided a rationalization for the use of (13) over a range of parameters which is physically meaningful and appropriate for the experimental reflection spectra under consideration. Of course, to be able to use (13) requires that we have the $\omega_{\mathbf{k}}$ values. These are eigenvalues of H_0 with $\Delta = 0$ plus H_1. As approximated they are shown in Fig. 11 for scalar k (transverse waves). How the dispersion curve was obtained and what to use for the general

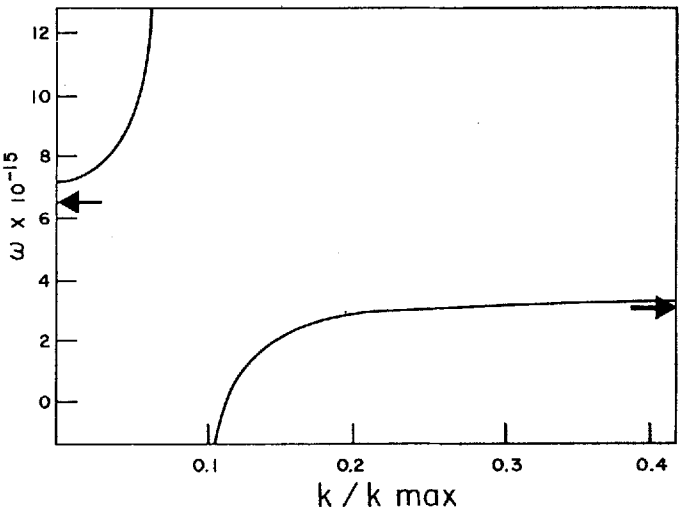

Figure 11. Theoretical dispersion curve calculated using retarded dipole–dipole interaction. Arrows refer to ω_- and ω_+ which would be found from Lorentz–Lorenz formula.

Downloaded by [Tomsk State University of Control Systems and Radio] at 06:13 17 February 2013

$\omega_{\mathbf{k}}$ will be discussed below and in Appendix B. In the next section mainly we show the result of using (13) in a practical calculation.

4. Theoretical Reflection Spectrum

In this section the theory is applied to the calculation of a reflection spectrum. Constants occurring in the formulas are for definiteness taken to match the experimentally determined single-molecule parameters and the crystal density for BDP ($\omega_0 = 24.4\,\text{kK}$, $\mu_y = 2.04\,\text{Å}$, and $\Delta = 1.9\,\text{kK}$). Thus one should be able, subject to appropriate qualification, to compare theory with experiment, i.e. Fig. 3 in Sec. 1.

The primary quantity to be computed is the susceptibility (7), which contains contributions from each transverse k mode. In the expression for a single contribution $\langle b_k(\tau) b_k^\dagger(0)\rangle_\omega$ (13) there is a sum which contains the three-dimensional exciton dispersion relation, $\omega(\mathbf{k})$. The one-dimensional dispersion relation for transverse excitons has been considered as determined for BDP (Appendix B and Fig. 11). Eventually we shall consider in some detail approximately how to obtain an estimate of the three-dimensional dispersion relation from the one-dimensional dispersion relation.

We can obtain a value for the expression (13) quickly if we are willing to make some rather drastic approximations, and this will constitute our first approach. (Subsequently we shall carry out the summation, in effect, exactly). To begin we can make the usual assumption that the longitudinal exciton energy effectively has no dispersion and that there is no interaction between the transverse and longitudinal modes. The $k = 0$ (transverse) already so to speak contains the longitudinal energy, and so each transverse ω_k may be considered as having this as an additive contribution. The sum over the 3-vector $\mathbf{k}$ can be replaced by a double sum over k_x and k_z (for the model the longitudinal modes are characterized by k_y) together with an appropriate factor.

The dispersion curve (Fig. 11) has two branches, split at the

Downloaded by [Tomsk State University of Control Systems and Radio] at 06:13 17 February 2013

value of k equal to k_0 (k_0 should go with ω_0 but see Appendix B). One sees that most of the modes have energies near the asymptotes ω_- and ω_+ of the branches. As an approximation, then, we can take all the levels on the lower branch to be at ω_- and all the levels on the upper branch to be at ω_+. One sees that by far most of the levels come at or near ω_-. The largest value of k on the upper branch should be given by the wavenumber for the single molecule transition, k_0 (reciprocal Compton wavelength). The largest k, $k_{\max}$, corresponds to a node every molecular plane, hence a wavelength corresponding to twice the thickness of a molecule. The ratio of the number of modes with energies near ω_- to the number with energies near ω_+ is therefore of the order of the Compton wavelength λ_0 divided by the lattice spacing $1/N^{1/3}$ or $k_{\max}/k_0 \approx \lambda_0 N^{1/3}$. For BDP this works out to be $\sim 10^3$. Referring to (13) we are here considering what might be called the main transverse part. For this part we shall assume that all the levels are either at ω_+ or ω_- in the ratio given above. We shall further assume that *all* the levels are at ω_- for the purpose of carrying out the sum over vector k.‡ With these two assumptions the susceptibility [equation (7)] becomes [through equation (13)]

$$\chi^*(\omega) = \chi(\omega) \approx (1 - 10^{-3}) N\mu_y^2 \times \left\{ \frac{1}{\omega_- + \gamma^2[1/(\omega - \omega_- - \Delta)] - \omega} + \frac{1}{\omega_- - \gamma^2[1/(\omega + \omega_- + \Delta)] + \omega} \right\} + 10^{-3} N\mu_y^2 \times \left\{ \frac{1}{\omega_+ + \gamma^2[1/(\omega - \omega_- - \Delta)] - \omega} + \frac{1}{\omega_+ - \gamma^2[1/(\omega + \omega_- + \Delta)] + \omega} \right\}$$

This expression is algebraically equivalent to the sum of four Sellmeier-type terms the more intense pair coming at $\omega_- + \frac{1}{2}\Delta(1 + 2^{-1/2})$ and $\omega_- + \frac{1}{2}\Delta(1 - 2^{-1/2})$ i.e. around ω_-, with

‡ Elementary consideration of the weights involved in the two-dimensional sum shows that the high k values, and hence ω_-, are especially favored.

Downloaded by [Tomsk State University of Control Systems and Radio] at 06:13 17 February 2013

a less intense pair (factor in the numerator of 10^{-3}) coming at $\omega_+ + \frac{1}{2}\Delta^2(\omega_+ - \omega_-)^{-1}$ and $\omega_+ + \Delta - \frac{1}{2}\Delta^2(\omega_+ - \omega_-)^{-1}$ i.e. around ω_+. To obtain this last result we have used the substitution $\gamma = \Delta/2$ (Sec. 3). Moreover the expressions for the frequencies around ω_+ have been simplified through the use of the strong

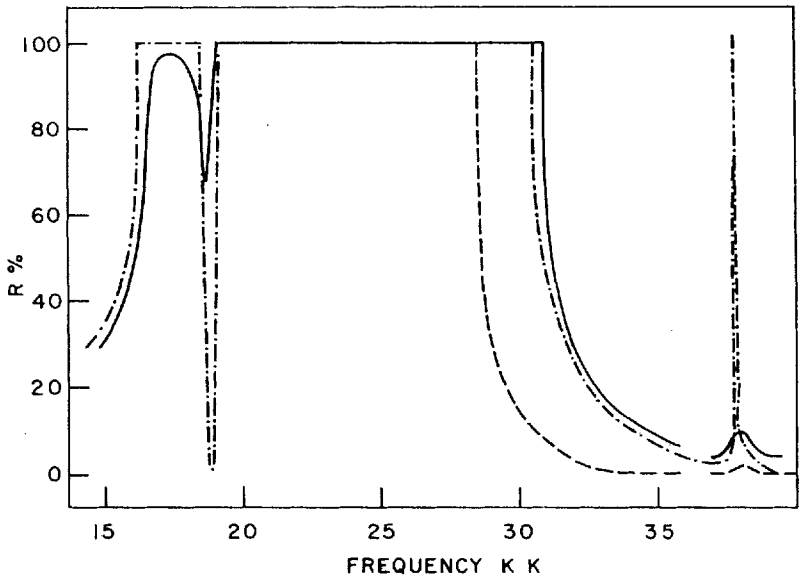

Figure 12. Theoretical reflection curves for 1,5-*bis*-(dimethylamino)pentamethinium perchlorate using exciton dispersion curve with levels at ω_- and ω_+ only (– · – ·), using full dispersion curve) (– – –) and (—) with and without consideration of higher transitions respectively. The solid and dashed curves have been magnified by a factor of ten in the region around 38 kK.

coupling criterion $\omega_+ - \omega_- \gg \Delta$. The reflection spectrum calculated from the susceptibility function above is given in Fig. 12 as the line with dots and dashes. In contrast with the result found from the Lorentz–Lorenz relation (see Sec. 1) there is structure not at ω_0 but at both ends of the stopping band. Also the position of the dip in the reflectivity near the low

Downloaded by [Tomsk State University of Control Systems and Radio] at 06:13 17 February 2013

frequency band edge is determined by the single molecule bandwidth and not the exciton band width.‡ Two essential features of the experimental reflection spectrum not given by this model are the observed deviation from 100% reflection and the depth of the dip at the low frequency edge. As $\chi(\omega)$ has been taken as real there is no absorption. However, we may now refine the calculation by making full use of the exciton dispersion curve. Damping (and hence absorption) is introduced, and in a way which, it is felt, is appropriately systematic.

We now go on to consider the complex susceptibility using as best we can the full exciton dispersion curve (i.e. we now approach the problem of the full summation in (13)). First we shall show how an estimate of the sum over vector k in (13) can be made using the transverse exciton dispersion relation. The contribution of the longitudinal excitons has already been mentioned. What remains is the double sum over k_x and k_z. The double sum may be replaced by a double integral.

With $N^{-1/3} = l$ the molecular diameter, and L the normalization box length we have $|n|$ in $\exp(2\pi inx/L)$ going from zero to $L/2l$ and $k_x = 2\pi n/L$ going from $-\pi/l$ to $\pi/l = \pi N^{1/3}$. The integral

$$\int_{-\pi/l}^{\pi/l}\int_{-\pi/l}^{\pi/l} S(k_x k_y)\, dk_x\, dk_y$$

(with arbitrary integrand S) can be approximated as

$$\int_0^{\sqrt{4/\pi}\,\pi/l}\int_0^{2\pi} S(k, \phi)\, d\phi\, k\, dk$$

‡ The fall-off in R at 30.7 kK does not occur at ω_+ (37.37 kK) because the width over which the index of refraction is imaginary is approximately $4\pi N\mu^2(2\omega_-)/\omega_- - \omega^2$ rather than the value given by the Lorentz–Lorenz theory: $4\pi N\mu^2(2\omega_0)/\omega_-^2 - \omega^2$. The small difference (large in reflectance) between these two expressions involves ω_p^4/ω_0^3 (using $\omega_- = \omega_0 - 1/3\omega_p^2/2\omega_0$) which is R^{-6} and may not be worth considering in a theory which does not properly put in van der Waals forces in the first place. All this, however, casts some doubt on the exactness of the prior empirical assignment for the front surface $\epsilon_{\text{total}} = \epsilon_{\text{effective}}$ (Eq. 9, Sec. 2 and footnote).

Downloaded by [Tomsk State University of Control Systems and Radio] at 06:13 17 February 2013

hence the double sum, in the known way, as

$$\left(\frac{L}{2\pi}\right)^2 \int_0^{\sqrt{4/\pi}\,\pi/l} \int_0^{2\pi} S(k, \phi)\, d\phi\, k\, dk$$

In the present instance we have the part of (13)

$$\frac{\gamma^2}{N} \frac{1}{\omega - \Delta - \omega_k}$$

becoming (now we put in the factor for the longitudinal modes, set $\omega' = \omega - \Delta$, and show the ϕ independence explicitly)

$$S(k, \phi) = \frac{\gamma^2}{N^{2/3}} \frac{1}{\omega' - \omega_k}$$

Thus our approximation for the sum in (13) becomes

$$\frac{1}{2\pi} \frac{\gamma^2}{N^{2/3}} \int_0^{\sqrt{4/\pi} \cdot \pi N^{1/3}} \frac{k\, dk}{\omega' - \omega_k}$$

(at this point we put $L = 1$).

In the case where there is singularity this integral is easily evaluated to give

$$i \frac{2\gamma^2}{\pi N^{2/3}} k(\omega_k = \omega') \left.\frac{dk}{d\omega_k}\right|_{\omega_k = \omega'}$$

In this expression as employed the values of k and the derivative are taken from the dispertion curve Fig. 11. At the singularities $\omega = \omega(k) + \Delta$ the damping is proportional to the density of states. From the dispersion curve it is easily seen that the damping and hence absorption is large near ω_- and to a lesser extent near ω_+. There are no singularities in the stopping band region between $\omega = \omega_- + \Delta$ and $\omega = \omega_+ + \Delta$. In this region the integral was evaluated numerically and leads to a level shift which is negligible except near $\omega_- + \Delta$. The reflection spectrum calculated from the

Downloaded by [Tomsk State University of Control Systems and Radio] at 06:13 17 February 2013

complex $\chi(\omega)$ (7) is the solid line in Fig. 12, our main result. (Compare the solid curve with the approximate curve obtained earlier—dots and dashes in Fig. 12).

The inclusion of the full dispersion curve has given remarkably good agreement between experiment and theory at the low frequency edge of the stopping band.‡ In contrast, the low flat reflectivity to the blue of ω_+ (Sec. 1) and the sharpness of the drop at the apparent ω_+ observed experimentally are not given especially well by the theory. However, the higher electronic transitions of the single molecule were not included in the calculation of the exciton dispersion curve. We can approximate the effect of the higher transitions by adding a small positive contribution to the real part of $4\pi\chi(\omega)$. The result of adding a background of 0.3 is shown in Fig. 12. Now the drop and the uniform low value for R to the blue of the high frequency band edge compare favorably with experiment.

We now return to a consideration of the absorption at the experimental high frequency band edge, Fig. 10. As mentioned above the theory predicts a large maximum in the absorption at ω_- and a much smaller one at $\omega_+ + \Delta$. If the experimentally observed high frequency fall off in the reflectance should in fact come at ω_+ then the singly resolved band§ may be assigned to the theoretically predicted transition at $\omega_+ + \Delta$. One reason why the theoretical ω_+ and theoretical drop-off point in R do not coincide has been given above. As a second reason—the effect of higher transitions should really have been considered directly in the calculation of the dispersion curve, not simply as an additive contribution to χ; one sees that if this were done properly the red shifted drop-off point in R would have going with it a red shifted ω_+.

‡ The height of the peak at the low frequency band edge decreases with smaller Δ. In those cases where the peak is low (Figs. 5, 6, 9) low phonon frequencies may be important.

§ In Fig. 10 the absorption to the blue may be attributed to higher single molecule transitions while the absorption to lower frequencies is undoubtedly related to the deviation from perfect reflection in the stopping band region.

Downloaded by [Tomsk State University of Control Systems and Radio] at 06:13 17 February 2013

Downloaded by [Tomsk State University of Control Systems and Radio] at 06:13 17 February 2013

Appendix A

Dynamical Equation for $g_k(\omega)$ Using the Two-Vibronic Level Hamiltonian

In this appendix we develop the dynamical equation for $g_k(\omega)$ using the two-vibronic level Hamiltonian (17). The commutator with the Hamiltonian involves commutation relations between exciton operators. It can be easily shown that the commutator for exciton momentum operators is

$$[b_k, b_{k'}^\dagger] = \delta_{kk'} - \frac{2}{N}\sum_l e^{il(k-k')}\, n_l$$

where $n_l = b_l^\dagger b_l$ is the number operator in position space.

Using this relation the commutator with the Hamiltonian is evaluated to give

$$[b_k, H] = \omega_k b_k - \frac{2}{N}\sum_{l,k'} \omega_{k'} e^{il(k-k')} n_l b_{k'}$$
$$- \frac{\Delta}{N}\sum_{q,q'} v_q^\dagger v_{q'}\left[b_{k+q-q'} - \frac{\Delta}{N}\sum_{k',l} e^{il(k-k')}\, n_l\, b_{k'+q-q'}\right]$$
$$+ \frac{\gamma}{\sqrt{N}}\sum_q (v_q + v_{-q}^\dagger)\left[b_{k-q} - \frac{2}{N}\sum_{k',l} e^{il(k-k')}\, n_l\, b_{k'}\right]$$

The effect of the exciton character of the operators is to bring in sums over the position number operator. In the corresponding Green's function $-i\theta(t)\langle[b_k(t), H]b_k^\dagger(0)\rangle$ these additional terms are zero as long as the ground state is the vacuum (i.e. the vacuum is an eigenfunction of the number operator with eigenvalue zero). Furthermore, the creation operator $v_q^\dagger$ operating to the left on the vacuum gives zero.

The dynamical equation for $g_k(\omega)$ then becomes

$$\omega\langle b_k(t)\, b_k^\dagger(0)\rangle_\omega = \langle b_k(0)\, b_k^\dagger(0)\rangle_\omega + \omega_k\langle b_k(t)\, b_k^\dagger(0)\rangle_\omega$$
$$+ \frac{\gamma}{\sqrt{N}}\sum_q \langle v_q(t)\, b_{k-q}(t)\, b_k^\dagger(0)\rangle_\omega \qquad \text{(A-1)}$$

In a similar manner one may derive the dynamical equation for the new Green's function:

$$\omega\langle v_q(t)\, b_{k-q}(t)\, b_k^\dagger(0)\rangle_\omega = [\omega_{k-q} + \Delta]\langle v_q(t)\, b_{k-q}(t)\, b_k^\dagger(0)\rangle_\omega + \frac{\gamma}{\sqrt{N}}\langle b_k(t)\, b_k^\dagger(0)\rangle_\omega - \frac{\Delta}{N}\sum_{q'}\langle v_{q'}(t)\, b_{k-q}(t)\, b_k^\dagger(0)\rangle_\omega + \frac{\gamma}{\sqrt{N}}\sum_{q'}\langle v_q(t)\, v_{q'}(t) b_{k-q-q'}(t) b_k^\dagger(0)\rangle_\omega \quad \text{(A–2)}$$

We may use the strong coupling result $(\gamma/\sqrt{N})\sum[\omega - \omega_{k-q} - \Delta]^{-1} \ll 1$ to eliminate the term $(\gamma/\sqrt{N})\sum_{q'}\langle v_{q'}(t)\, v_{q'}(t)\, b_{k-q'-q}(t)\, b_k^\dagger(0)\rangle_\omega$. Then if the Δ/N term in the above equation is neglected we recover the simple result which one obtains with the tentative Hamiltonian (12) i.e.

$$\langle v_q(t)\, b_{k-q}(t)\, b_k^\dagger(0)\rangle_\omega = \frac{\gamma}{\sqrt{N}}\frac{\langle b_k(t)\, b_k^\dagger(0)\rangle_\omega}{\omega - \omega_{k-q} - \Delta} \quad \text{(A–3)}$$

To test whether the Δ/N term in A–2 can be neglected we substitute the expression A–3 into the sum in A–2 and obtain

$$\langle v_q(t)\, b_{k-q}(t)\, b_k^\dagger(0)\rangle_\omega = \frac{\gamma/\sqrt{N}}{\omega - \omega_{k-q} - \Delta}\left\{\langle b_k(t)\, b_k^\dagger(0)\rangle_\omega\left[1 - \frac{\Delta}{N}\sum_q(\omega - \omega_{k-q} - \Delta)^{-1}\right]\right\} \approx \frac{\gamma/\sqrt{N}\,\langle b_k(t)\, b_k^\dagger(0)\rangle_\omega}{\omega - \omega_{k-q} - \Delta}$$

Equations A–1 and A–3 are solved to give

$$\langle b_k(t)\, b_k^\dagger(0)\rangle_\omega = \left\{\omega - \omega_k - \frac{\gamma^2}{N}\sum_q[\omega - \omega_{k-q} - \Delta]^{-1}\right\}^{-1}$$

which is the same result (13) as would be obtained with the Hamiltonian (12).

Downloaded by [Tomsk State University of Control Systems and Radio] at 06:13 17 February 2013

Appendix B

Approximate Dispersion Curve

We need to obtain ω_k or equivalently the perturbation energy $\omega_k - \omega_0$ (where k is the scalar wave number k_z) for parallel transition moments μ_y on a cubic lattice interacting through the retarded Coulomb interaction. Initially let us consider the $k = 0$ mode and assume that the dipoles interact simply through the instantaneous Coulomb interaction. With $k = 0$ the perturbation energy reduces to a sum of contributions

$$-\mu \sum_i \epsilon_i = -\mu_y \sum_i \epsilon_{yi}$$

where, for the instantaneous interaction

$$\epsilon_{yi} = \frac{\mu_y G_i}{R_i^3}$$

Here G_i is the well-known trigonometric factor, proportional to $P_2(\theta)$, and θ is the angle between y and the radius vector $\mathbf{R}_i$.

The perturbation energy is then the energy of a representative dipole at the origin in the field of the others. $\vec{\epsilon_i}$ is thus the contribution to the field at the origin coming from the ith dipole. We shall be using the procedure of actually summing such contributions. This is feasible if we employ an approximation. The above way of looking at the problem perhaps best facilitates understanding the approximate procedure chosen: Collect together all transition dipoles in a cube, j, containing p dipoles and relocated at an appropriate point in the cube, and take $\mathbf{R}_j$ as the radius ve tor to this point in the cube. Then each partial sum referring to the dipoles in the jth collection

$$\sum_{i=1}^{p} \epsilon_{yi} \approx \frac{(p\mu_y)G_j'}{R_j'^3}$$

(R_j' and G_j' being sufficiently close to the several R_i and G_i). Thus for the $k = 0$ mode an approximation would be to consider that there are supermolecules (labelled j) on a lattice with spacing

Downloaded by [Tomsk State University of Control Systems and Radio] at 06:13 17 February 2013

increased by $p^{1/3}$, each with moment $p\mu_y$. A sum over supermolecules j should reproduce most if not all of the essential features in the sum over the molecules i. The representative molecule at the origin would remain as an ordinary molecule with transition moment μ_y—for the purpose of the calculation of the perturbation energy.

What is more, if one takes R_j' as going to the far corner of each cube, each term

$$\frac{(p\mu_y)G_j'}{R_j'^3} = \frac{(p\mu_y)G_j'}{(p^{1/3}R_j)^3} = \frac{\mu_y G_j'}{R_j^3} = \frac{\mu_y G_j}{R_j^3}$$

this provided that the j of R_j is associated with the j of R_j' in an obvious way (which is made possible by the congruence between the first lattice and the lattice of supermolecules.) If the infinite sum were to converge the approximation would be exact.

We are interested in not the instantaneous Coulomb interaction but the retarded Coulomb interaction. The R dependence is not all R^{-3}. Also we are interested in all the transverse k modes from $k = 0$ to $k = k_{\max}$ (180° phase reversal in each succeeding molecular plane). Keeping to the case of the instantaneous interaction let us now examine the $k_{\max}$ case. In general, when $k \neq 0$ one has to assign phases to the ϵ_i's, as expected, but also one must not forget to average suitably over phase for the molecule at the origin—the perturbation energy as a diagonal matrix element is a double sum. Let us look at the sum over ϵ_i's as if the phase of the representative molecule were not important. The jth partial field at the origin now may be represented thus

$$\epsilon_j = \frac{\mu_y G_j F_j}{R_j^3}$$

where F_j is ± 1 depending on whether the plane containing the transition dipole is even or odd (as numbered serially along the z axis). But reversing the reasoning above this becomes

$$\frac{(p\mu_y)G_j'F_j'}{R_j'^3}$$

where there is a 180° phase reversal every plane of supermolecules.

Downloaded by [Tomsk State University of Control Systems and Radio] at 06:13 17 February 2013

Whether we use molecules or supermolecules the perturbation energy comes out the same, as long as the potential is R^{-3}. What reason to use supermolecules?

We wish to employ complicated phase factors which give not only a plane exciton wave along z but spherical waves with wave vector k_0 (going with ω_0) radiating out from the representative molecule at the origin (retardation spheres). We also need to carry out the sum over a macroscopic section of crystal, which means including quite a few retardation spheres. Now k_0 corresponds to the wavelength of light which excites the single molecule transition, 4000 Å, and the lattice spacing is 4 Å. The number of molecules in a single retardation sphere is thus of the order of 1000^3 and it is for this reason more convenient to sum over supermolecules.

In order to delineate the sinusoidal shape of a retardation sphere we adopted the plan of taking six points every half wavelength along a radius. Thus we shall be dealing with a lattice spacing of about 4000/12 (Å) or alternatively an ω_0 having a Compton wavelength of ~330 Å in the first place. Another point of view is simply that we are using a sum over supermolecules having a size which would give the requisite lattice spacing. This way the work involved in doing the lattice sum by brute force on the computer is kept within bounds. The final result is probably reasonably satisfactory at $k = 0$, and $k = k_{max}$ (though the retarded interaction is not all R^{-3}) but it turns out not to be satisfactory at a value of $k = k_0$ ($k_z = k_0$). The situation is that the perturbation method goes bad at $k = k_0$, the upper branch of $\omega(k)$ going to $+\infty$ and the lower to $-\infty$. The ω_+ and ω_- branches join, so to speak, at ∞. When the ordinary sum is used, as mentioned in the text, this result is the number of states on the upper branch to the total number, (or essentially that on the lower branch) being in the ratio λ_{min}/λ_0 or $k_0/k_{max} \approx 1/1000$. When the supermolecule method is used k_{max} is much reduced with respect to k_0. The k_{max} on the new scale has a phase turnover every supermolecule, As explained above, this should not give a poor value for the $\omega(k)$ at the real k_{max}. Thus we may attempt to

Downloaded by [Tomsk State University of Control Systems and Radio] at 06:13 17 February 2013

use a linear scale of k which terminates at the k_{max} of the new scale as if it were the actual k_{max}, but with this procedure the dispersion curve on the lower branch plunges to $-\infty$ at the wrong k_0. Admittedly, leaving much to be desired, this is to be our dispersion curve.

The y component for the partial field at the origin was in the present research taken as[7]

$$\epsilon_{yi} = \mathrm{Re}\left[-\mu_y \left(\frac{\partial^2}{\partial x^2} + \frac{\partial^2}{\partial y^2} \right) \frac{e^{-ik_0 R_i}}{R_i} \right] F_i$$

In summing, as many as 300^2 lattice points per xy plane were included. Then various planes were brought in with the F's governed by k. As many as 600 planes were included. The result was convergent in the sense that an undulating value for $\omega(k)$ with period corresponding to k_0 eventually reproduced itself. Values of $\omega(k)$, shown in Fig 11, correspond to an average over these undulations. Averaging was carried out by increasing the size of an xy plane and at the same time increasing the number of planes in the z direction. The asymptotic values come, gratifyingly, within the error of the numerical approximations employed, at the ω_+ and ω_- of the Lorentz–Lorenz formula.‡

To match BDP, k_0 was taken as 1.4×10^5 (corresponding to a single molecule peak absorption of 4090Å) and μ_y as corresponding to a transition moment length of 2.0Å (one-dimensional oscillator strength of 3.3 or plasma frequency-squared of $\omega_p^2 = 32.9 \times 10^{30}$).

‡ The undulations could be a manifestation of that field which comes from the surface charges to cancel the penetrating incident field (extinction theorem). We are not sure about this point, for one reason because we are not sure that we have used the right boundary conditions at the surfaces.

REFERENCES

1. Anex, B. G. and Simpson, W. T., *Revs. Mod. Phys.* **32**, 466 (1960). For an up-to-date theoretical treatment, see McLachlan, A. D., and Ball, M. A., *Mol. Phys.* **8**, 581 (1964).
2. K. Huang, in M. Born and K. Huang, *Dynamical Theory of Crystal Lattices* (Oxford University Press, London, 1954), Chapter 7.

Downloaded by [Tomsk State University of Control Systems and Radio] at 06:13 17 February 2013

3. Hopfield, J. J., *Phys. Rev.* **112**, 1555 (1958); and Fano, U., *Phys. Rev.* **203**, 1202 (1956).
4. Haas, G., Hunter, W. R., and Tonsey, R., *Jour. Opt. Soc. Am.* **46**, 1009 (1956).
5. Dyson, J., *Proc. Phys. Soc. B*, **62**, 565 (1949).
6. Credit for the pioneer work seems to center around Migdal and Galitskii's paper on Green's functions and the work on the fluctuation dissipation theorem by Kubo. This approach has been undergoing development by a large number of workers. For a review see Zubarev, D. N., *Soviet Phys.-Usp.*, 320 (1960).
6a. For a useful treatment specifically involving excitons, see also Rhodes, W., and Chase, M., *Revs. Mod. Phys.* **39**, 348 (1967) and references therein.
7. Simpson, W. T., *Rad. Res.* **20**, 87 (1963); see also McClone, R. R., and Power, E. A., *Mathematika* **11**, 91 (1964).
8. Frohlich, H., *Proc. Roy. Soc.* (London) **215A**, 291 (1952).
9. Suna, A., *Phys. Rev.* **135**, A111 (1964).

Downloaded by [Tomsk State University of Control Systems and Radio] at 06:13 17 February 2013